Color Tunable Phosphorescent Neutral Manganese(II) Complexes through Steric Hindrance Driven Bond Angle Distortion

Pengfei She, Zhong Zheng, Yanyan Qin, Feiyang Li, Xiaokang Zheng, Dongdong Zhang, Zhiyuan Xie, Lian Duan* and Wai-Yeung Wong**

Dr. P. She, Dr. Y. Qin, X. Zheng, Prof. W.-Y. Wong

Department of Applied Biology and Chemical Technology and Research Institute for Smart Energy. The Hong Kong Polytechnic University, Hung Hom, Hong Kong P. R. China and The Hong Kong Polytechnic University Shenzhen Research Institute, Shenzhen 518057, P. R. China.
Email: wai-yeung.wong@polyu.edu.hk

Z. Zheng, Dr. D. Zhang, Prof. L. Duan
Key Lab of Organic Optoelectronics and Molecular Engineering of Ministry of Education, Department of Chemistry, Tsinghua University, Beijing 100084, P. R. China.
Email: duanl@mail.tsinghua.edu.cn

Dr. F. Li
School of Environmental and Chemical Engineering, Jiangsu University of Science and Technology, Zhenjiang 212100, P. R. China

Prof. Z. Xie
State Key Laboratory of Polymer Physics and Chemistry, Changchun Institute of Applied Chemistry, Chinese Academy of Sciences, Changchun 130022, P.R. China

Keywords: crystal field strength, color tunable manganese(II) complexes, steric hindrance, bond angle distortion, organic light-emitting diodes

Phosphorescent manganese(II) complexes with high photoluminescence quantum yields (PLQYs) and low cost exhibit great potential in organic light-emitting diodes (OLEDs), information security and X-ray imaging. However, it is still a challenge to tune their emission colors. Herein, an effective strategy for engineering the phosphorescence colors of tetrahedral Mn(II) complexes through steric hindrance driven bond angle distortion is proposed. Modulating the steric hindrance between phosphine and benzofuran and varying the O-Mn-O

bond angles allows these Mn(II) complexes to emit from 498 nm to 548 nm. Interestingly, these achiral Mn(II) complexes exhibit significant CPL signals due to symmetry breaking. Furthermore, high-performance green OLEDs are achieved by using these Mn(II) complexes as dopants, providing a record-high external quantum efficiency of 15.7%. These super-duper results greatly inspire the development of multi-color Mn(II) complexes and low-cost Mn-based devices.

1. Introduction

Phosphorescent transition metal complexes, such as iridium(III), platinum(II) and gold(III) complexes etc., have recently attracted significant interest due to their tunable photophysical properties including emission intensity, color, and lifetime.[1-5] Consequently, these materials have been well exploited and widely used in various optoelectronic applications.[6-10] However, these noble metals exhibit the low abundance and high cost. Phosphorescent manganese(II) complexes, as an emerging class of luminescent materials with high photoluminescence quantum yields (PLQYs), low cost and toxicity, as well as easier synthesis, have exhibited exceptional performance in organic light-emitting diodes (OLEDs),[11-14] information security, [15-17] X-ray imaging[18-22] and opto-electronic switches.[23] Nevertheless, the tuning of the intrinsic emission colors of Mn(II) complexes remains a big challenge because of the inherent Mn-center d-d ($^4T_1(G)$-$^6A_1$) radiative transition feature. Furthermore, Mn emission is highly dependent on the crystal field strength,[24-26] and a stronger crystal field strength could induce weaker separation between the $^4T_1$ and $^6A_1$ levels, resulting in a shift of the emission peak towards lower energies (**Figure 1**a). Therefore, octahedrally coordinated Mn(II) complexes with strong crystal field strength usually display red-shifted emission than tetrahedrally coordinated Mn(II) complexes. However, little attention has been paid to the controllable modulation of emission colors of octahedrally or tetrahedrally coordinated Mn(II) complexes at their confined coordination numbers. To date, the strategy based on varying heavy atoms has become the most universal method to control the crystal field strength of tetrahedral Mn center.[27-29] In contrast, organic ligands, as important components in Mn(II) complexes that also play a significant role in influencing the crystal field strength in theory, are seldom considered for effectively modifying the emission colors of the Mn center.

Considering that the crystal field strength of Mn center is related to the bond angle distortion,[30-31] we envision that the control of steric hindrance of organic ligand could be an effective strategy to regulate the distance of coordination sites, and further tune the bond angle

distortion for multi-color Mn center emissions. Recently, it has been shown that phosphine oxide ligands play a key role in constructing various neutral mono- or bidentate Mn(II) complexes.[32-34] Particularly, bidentate phosphine oxide ligands with tunable steric hindrance effect between the rigid backbone and phosphine oxide moiety could be used to regulate the bond angle distortion of Mn center and influence its coordination environment. However, the P=O sites of reported bidentate phosphine ligands are fixed in the same positions of benzofuran derivatives and the corresponding Mn(II) complexes exhibit similar Mn center coordination environment and emission color.[35] Meanwhile, according to the Dexter's exchange mechanism, shortened donor−acceptor distance and appropriate organic ligand energy levels will contribute to the adjustment of the ligand-metal centered energy transfer process.[36-37] Therefore, it is worth exploiting the use of bidentate phosphine ligands with different intramolecular steric hindrance for the regulation of bond angle distortion and crystal field strength, which may significantly tune the emission color and PLQY, and decipher the structure−property relationship of Mn(II) complexes.

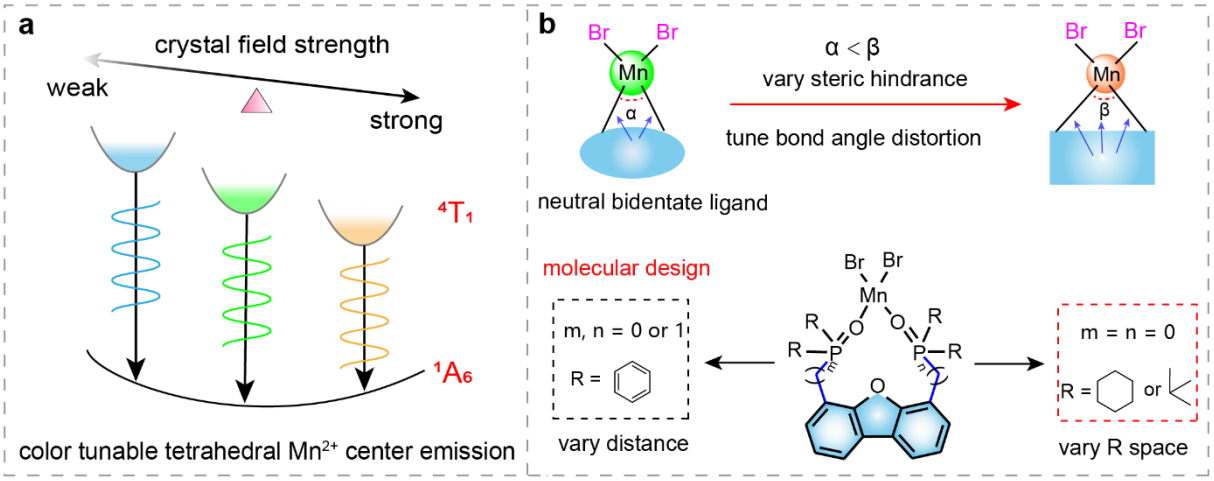

Figure 1. a) Proposed mechanism for tunable emission of Mn center. b) Steric hindrance driven bond angle distortion behavior and molecular structures of designed Mn(II) complexes.

To validate our hypothesis, five bidentate phosphine oxide ligands with benzofuran unit were designed and synthesized (Figures 1b, S1-S20 and Scheme S1-S3, Supporting Information), and then chelated with manganous bromide to form neutral tetrahedral Mn(II) complexes. The obtained Mn(II) complexes were well characterized by single crystal X-ray diffraction. As anticipated, different steric hindrance effects by varying the phosphine-benzofuran distance make the Mn center emission peaks shift from 498 to 548 nm, accompanied by changes in the luminescence color from blue-green, green to yellow-green. Interestingly, these achiral Mn

single crystals also exhibited significant circularly polarized luminescence (CPL) signals. Thus, by using these Mn(II) complexes with high PLQYs as emitters, green OLEDs were successfully fabricated with a maximum current efficiency (CE_{max}) of 48.1 cd A^{-1}, power efficiency (PE_{max}) of 53.9 lm W^{-1}, and external quantum efficiency (EQE_{max}) of 15.7%.

2. Results and Discussion

At first, three bidentate phosphine oxide ligands (DMePO, MePO and DPhPO) were synthesized through incorporating diphenylphosphine oxide homologue into benzofuran. Then, the bidentate phosphine oxide ligands reacted with an equal equiv. of $MnBr_2 \cdot 4H_2O$ in the solvent mixture of ethanol and dichloromethane at room temperature to afford the target neutral Mn(II) complexes. Crystals of the Mn(II) complexes were prepared by a simple diffusion method. Impressively, the as-prepared single crystals of Mn(II) complexes displayed different luminescence colors from blue-green, green to yellow-green under 365 nm UV light (**Figure 2**a), indicating that the regulation of organic ligands for the control of emission color of Mn(II) complexes is possible.

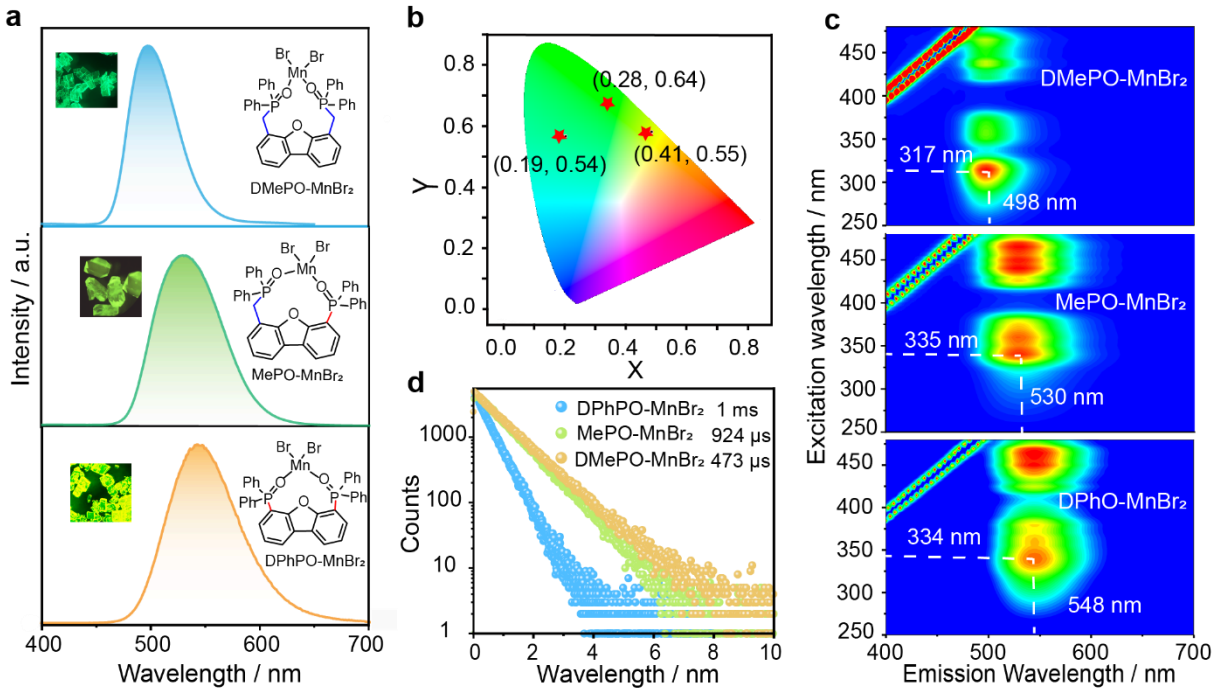

Figure 2. a) Normalized luminescence spectra and the related photographs of DMePO-$MnBr_2$, MePO-$MnBr_2$, and DPhPO-$MnBr_2$, respectively. b) CIE chromaticity coordinate diagram of the luminescence color of three Mn(II) complexes. c) Excitation-emission mapping of three Mn(II) complexes. d) Lifetime decay curves of emission bands at 498, 530, and 548 nm for DMePO-

$MnBr_2$, MePO-$MnBr_2$, and DPhPO-$MnBr_2$, respectively.

Next, the photophysical properties of Mn(II) complexes were investigated in detail to understand the nature of the color tunable luminescence behaviors. As shown in Figure 2a, DMePO-$MnBr_2$ presents the main emission peak at around 498 nm, while MePO-$MnBr_2$ and DPhPO-$MnBr_2$ display emission peaks at 530 and 548 nm, respectively, which originate from the characteristic radiative transition between $^4T_1$ and $^6A_1$ of Mn center. The corresponding Commission International de l'Eclairage (CIE) coordinates of (0.19, 0.54), (0.28, 0.64) and (0.41, 0.55) are distributed in the obviously different regions (Figure 2b). Upon excitation by different wavelengths, no changes can be observed in the luminescence spectral profiles (Figure 2c). It is worth noting that the change in emission wavelength of nearly 50 nm is found in our designed Mn(II) complexes, belonging to the widest emission color changes to date in contrast to that tuned by the reported heavy atom strategy, to the best of our knowledge. Moreover, their luminescence excitation spectra consisted of three similar bands. Taking DMePO-$MnBr_2$ as an example, the first broadband with high intensity located at ~250−340 nm originate from the absorption of organic ligand, which can transfer the absorbed energy to the Mn center. The other two broad bands, what are located at ~350 nm to 400 nm and ~430 nm to 480 nm, are assigned to the transitions of G state and D state of the Mn center (Figure S21, Supporting Information). Additionally, under the excitation of about 320 nm, DMePO-$MnBr_2$, MePO-$MnBr_2$ and DPhPO-$MnBr_2$ are well fitted with a mono-exponential decay lifetimes of 475 μs, 925 μs, 1 ms and high PLQYs of 50.3%, 75.2%, and 83.0%, respectively (Figure 2d and Table S1, Supporting Information). Notably, the variation of their emission lifetimes follows the same trend as their PLQYs, with DPhPO-$MnBr_2$ showing the highest PLQY and the longest lifetime. Based on the above results, we speculate that slight regulation of organic ligands could greatly influence the coordination environment of Mn center and change the intramolecular energy transfer efficiency, providing an effective strategy for on-demand engineering of the emission color, lifetime as well as PLQY.

To prove this conjecture, we conducted a single crystal analysis on the three Mn(II) complexes. As shown in **Figures 3**a-c, these Mn(II) complexes exhibit a distorted tetrahedral coordination environment, with the Mn atom coordinated by two Br and two O atoms from the phosphine oxide moiety, forming a robust zero-dimensional distorted structure. From these single crystal structures, it is evident that the benzofuran group, as a large conjugation unit, exerts significant steric hindrance in modulating the O_1-O_2 distance. Consequently, a longer O_1-O_2 distance may result in a larger O_1-Mn-O_2 bond angle. For instance, due to the long

distance between the benzofuran group and P=O units, DMePO-$MnBr_2$, which has weak steric hindrance, exhibits an O_1-O_2 distance of 3.2 Å and an O_1-Mn-O_2 bond angle of 104.7º, whereas MePO-$MnBr_2$ and DPhPO-$MnBr_2$, which have longer O_1-O_2 distances, display the bigger corresponding O_1-Mn-O_2 bond angles of 114.5º and 122.2º, respectively. Therefore, we speculated that adjusting the steric hindrance between benzofuran group and P=O units could regulate the distance between O_1 and O_2, thereby achieving the predictable O_1-Mn-O_2 bond angle. We then examined their independent gradient model (IGM) for assessing the difference in steric hindrance by comparing the intramolecular attractive and repulsive interactions.[38] As displayed in Figures 3d-g and S22, Supporting Information, the green iso-surface is observed between the Mn and the surrounding aromatic units, indicating weak attractive interactions. Compared with DMePO-$MnBr_2$ and MePO-$MnBr_2$, effective repulsive interactions are observed between the phosphine oxygen bond and benzofuran unit in DPhPO-$MnBr_2$, as indicated by the red iso-surface regions. This also demonstrates the existence of strong steric hindrance in DPhPO-$MnBr_2$. Meanwhile, their bond angle variances are 9.74-, 21.91- and 64.52-degree square, respectively (Figure 3h), which are consistent with the degree of steric hindrance.

According to the prior research, crystal field strength is related to bond distortion, and increased distortion would lead to stronger crystal field splitting.[30] Therefore, we assessed the degree of splitting by utilizing the discrepancy between excitation peak ($^6A_1 \rightarrow {}^4T_2$) and emission peak ($^4T_1 \rightarrow {}^6A_1$).[27] As shown in Figure 3i, DPhPO-$MnBr_2$ has the largest value of $E[^4T_2] - E[^4T_1]$ (0.57 eV), which corresponds to the stronger ligand field, whereas the values of $E[^4T_2] - E[^4T_1]$ for MePO-$MnBr_2$ and DMePO-$MnBr_2$ are 0.34 and 0.50 eV, respectively, which belong to the relatively weak ligand field. Therefore, DPhPO-$MnBr_2$, which has a big bond angle distortion value, displays a stronger crystal field strength, together with a red-shifted emission peak at 548 nm. As a whole, steric hindrance driven bond angle distortion is an effective strategy for engineering crystal field strength and emission color.

To gain a deep insight into the luminescence properties of these Mn(II) complexes, the time-dependent density functional theory (TDDFT) calculations were also carried out. It is worth noting that all LUMOs are mainly located at the Mn center and two Br atoms, while all $HOMO_S$ comprise atomic orbitals of benzofuran unit (Figure S23, Supporting Information). The obvious charge transfer nature suggests that the benzofuran unit in organic ligand may play a crucial role in mediating the energy transfer between ligand and Mn center. The short distance between benzofuran unit and Mn center contributes to the energy transfer efficiency in accordance with the Dexter rule, thereby further enhancing the PLQY and prolonging the emission lifetime of

these Mn(II) complexes. Thus, by controlling the intramolecular steric hindrance, the emission color of Mn(II) complexes could be regulated, and their emission lifetime, PLQY as well as thermal stability could be modulated (Figure S24, Supporting Information).

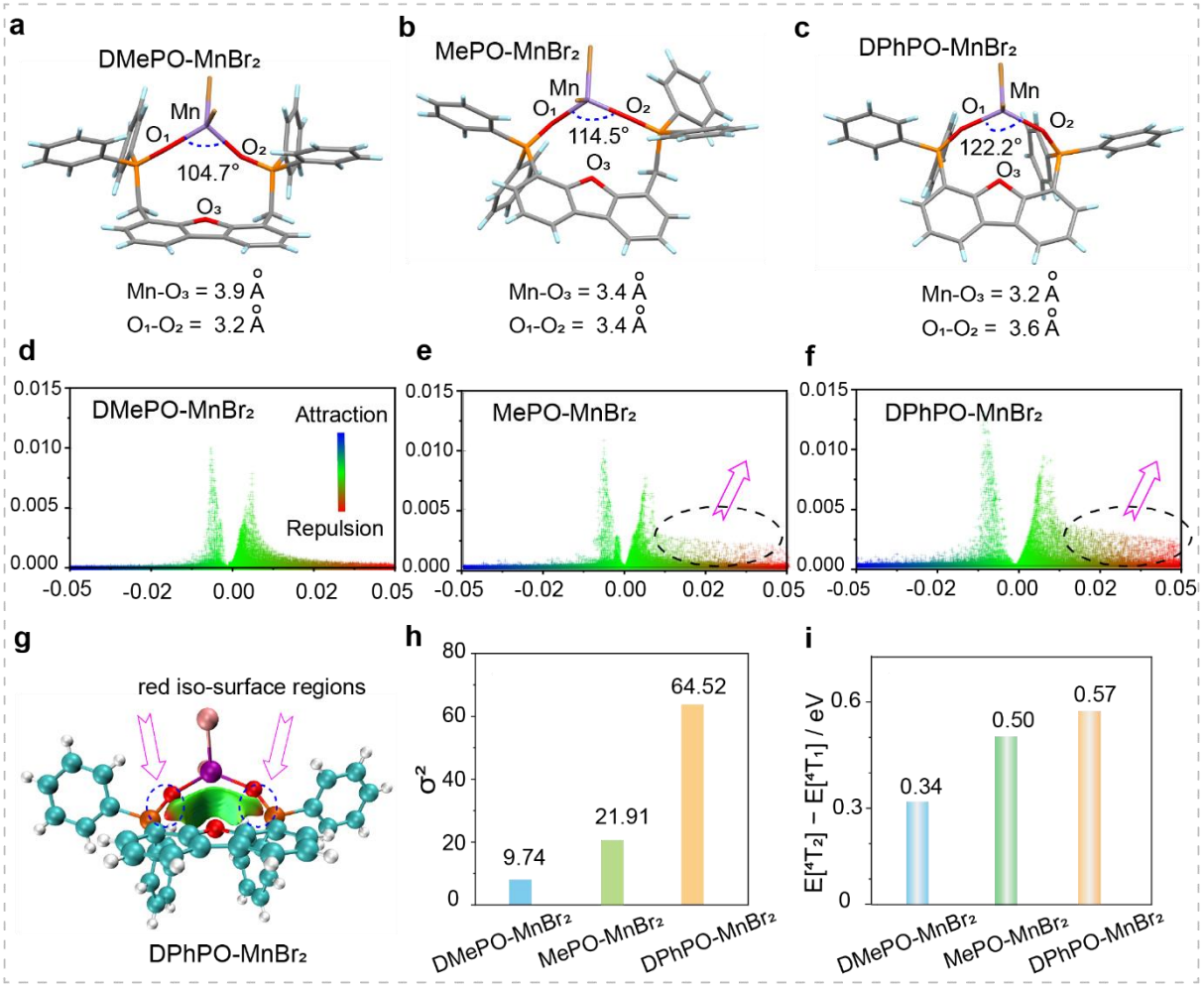

Figure 3. a-c) Single crystal structure analysis of DMePO-$MnBr_2$, MePO-$MnBr_2$, and DPhPO-$MnBr_2$, respectively. d-f) The 2D scatter plot with a black circled spike. g) The local 3D noncovalent interaction plot of DPhPO-$MnBr_2$ with an iso-surface value of 0.5 a.u. h) The calculated bond angle distortion values. i) The difference between optical bands E[$^4T_2$] and E[$^6A_1$] to reflect the strength of the crystal field.

To further validate the proposed color-tuning mechanism, we prepared two control molecules, DcycPO-$MnBr_2$ and DtbuPO-$MnBr_2$, to regulate the crystal field strength of Mn center (**Figure 4**a), in which adjacent cyclohexyl units with large spatial volume can exhibit a stronger steric hindrance effect than the tert-butyl and benzene rings. As shown in Figure 4b and c, DcycPO-$MnBr_2$ exhibits obvious intramolecular distortion between P and benzofuran part (Figure S25, Supporting Information), which enlarges the O_1-O_2 distance (3.46 Å) to result in a bigger O_1-

Mn-O_2 bond angle than DtbuPO-$MnBr_2$. Differently, due to the synergistic effect of π-π interaction of adjacent benzene and steric hindrance, DPhPO-$MnBr_2$ presents the biggest bonding angle among these Mn(II) complexes. Thus, DcycPO-$MnBr_2$ and DtbuPO-$MnBr_2$, which have small bond angle distortion values, display small energy splitting and blue-shifted emission peaks at 531 and 537 nm (Figure 4d). Importantly, DcycPO-$MnBr_2$ and DtbuPO-$MnBr_2$ exhibit the enhanced PLQY of 90% and 85%, respectively, as well as slightly long emission lifetimes. This is because their short donor−acceptor distance can contribute to the high energy transfer efficiency (Figure S26, Supporting Information).

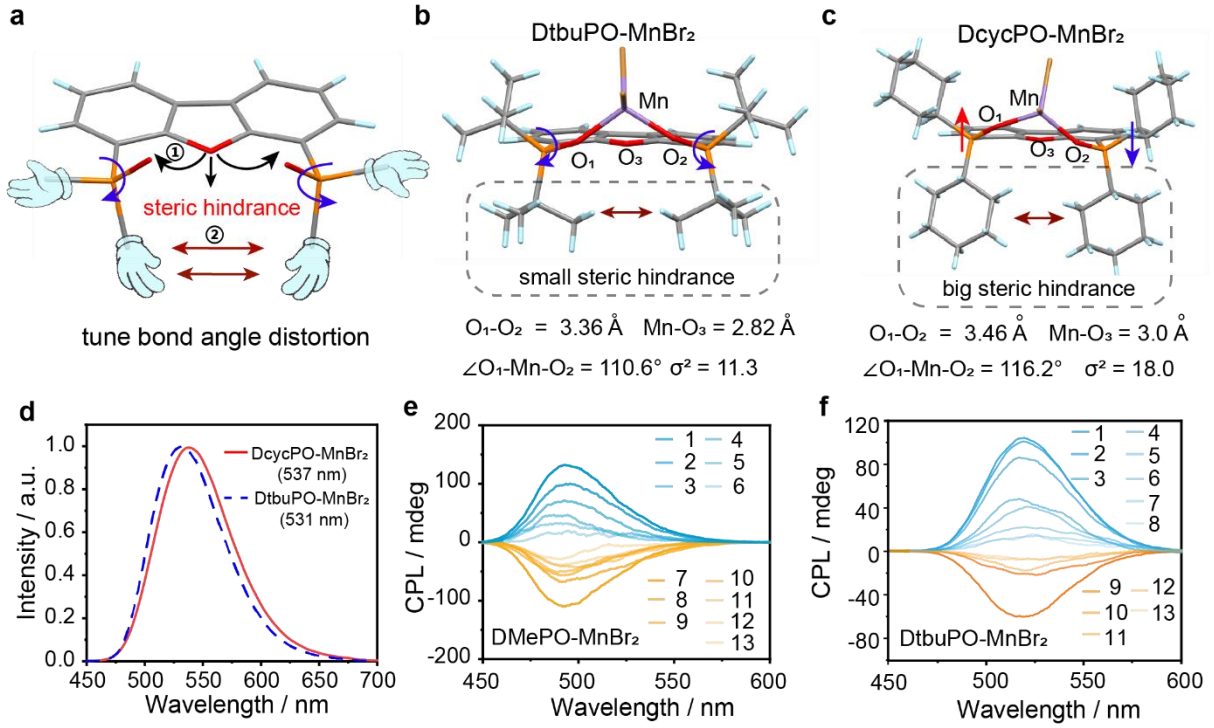

Figure 4. a-c) The Single crystal structure analysis and the corresponding bond angle distortion values. d) Luminescence spectra of DcycPO-$MnBr_2$ and DtbuPO-$MnBr_2$. e-f) CPL spectra of DMePO-$MnBr_2$ and DtbuPO-$MnBr_2$.

Surprisingly, we found that these Mn(II) complexes exhibited significant CPL signals. For example, DMePO-$MnBr_2$ single crystals were randomly picked out, and then their CPL signals were tested (Figure 4e). In a total of 13 trials, six samples displayed positive CPL signals and seven samples showed negative CPL signals. This result may be attributed to the anisotropic optical activity of achiral crystals. Like DMePO-$MnBr_2$, the other four Mn(II) complexes also showed this CPL behavior due to symmetry breaking (Figures 4f, S27 and S28, Supporting Information).[39-41] Notably, the point groups of these Mn(II) complexes are $\bar{1}$, 2/*m* and *mmm*

(Scheme S4 and Table S2, Supporting Information), which do not belong to the four reported achiral point groups, ($\bar{4}2m$ (D_{2d}), $\bar{4}$(S_4), $mm2$ (C_{2v}), and m (C_s)). Therefore, these unique CPL properties exhibited by these Mn(II) complexes not only broaden the range of materials with CPL properties, but also offer a new direction for implementing CPL activities of crystals in achiral space groups.

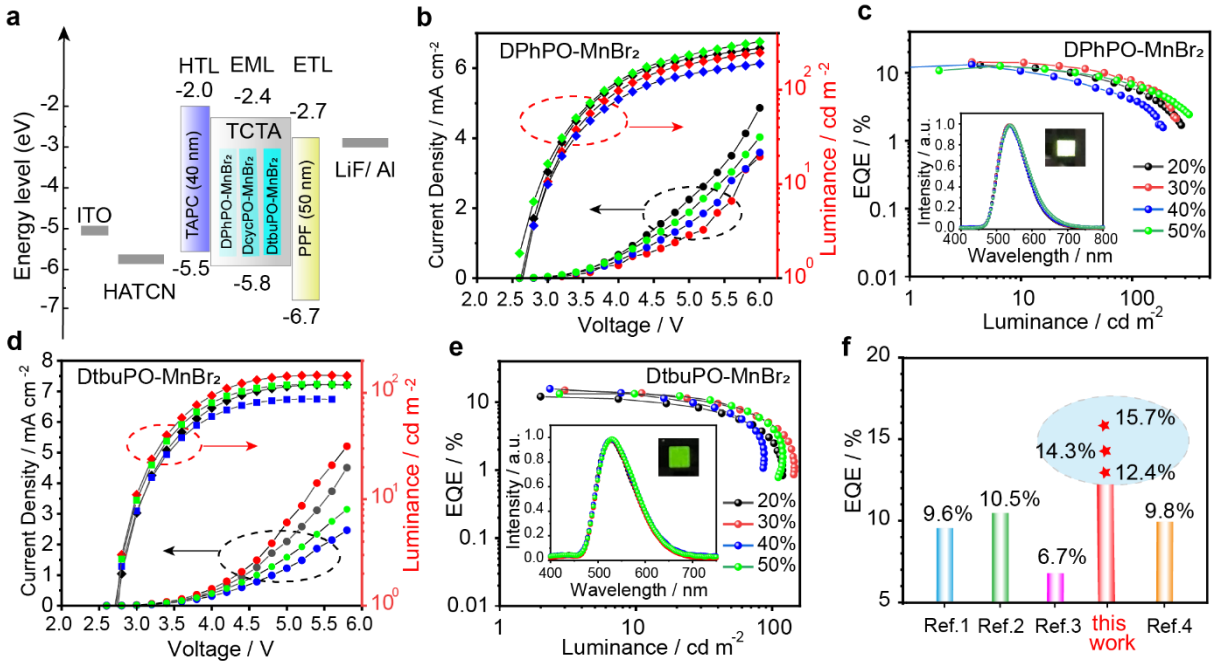

Figure 5. a) Device configuration with energy-level diagram. b-e) Current density-voltage-luminance and EQE- luminance curves of devices based on DPhPO-$MnBr_2$ and DtbuPO-$MnBr_2$, inset of c and e: EL spectra of devices based on DPhPO-$MnBr_2$ and DtbuPO-$MnBr_2$ and the photographs showing the emission color of the device at 40 wt% doping concentration. f) The EQE comparison of reported Mn(II)-based devices and this work.

The electroluminescence (EL) properties of these neutral Mn(II) complexes were investigated by fabricating OLEDs using DPhPO-$MnBr_2$, DcycPO-$MnBr_2$ and DtbuPO-$MnBr_2$ as the representative emitters due to their better photophysical properties. The experimental HOMO and LUMO energy levels for three Mn(II) complexes are summarized in Table S3, Supporting Information. The conventional host 4,4′,4″-*tri*(9-carbazolyl)-triphenylamine (TCTA) was utilized for these phosphorescent devices because of its large band gap (E_g = 3.4 eV) and good charge transporting capability.[42] As displayed in **Figure 5**a, the vacuum deposited OLED structures consist of ITO/ HATCN (3 nm)/ TAPC (40 nm)/ TCTA: x wt % Mn emitters (24 nm)/ PPF (50 nm)/ LiF (1 nm)/ Al (120 nm), in which

hexaazatriphenylenehexacabonitrile (HATCN) and lithium fluoride (LiF) act as the hole-injecting and electron-injecting layers, and tris[4-(carbazol-9-yl)phenyl]amine (TAPC) and 2,8-Bis(diphenylphosphoryl)dibenzo[b,d]furan (PPF) serve as the hole transporting and electron-transporting layers, respectively. The molecular structures of the utilized materials in the device are shown in Figure S29, Supporting Information.

Upon increasing the dopant concentration from 20% to 50%, all doped devices show a very low turn-on voltage (V_{on}) of 2.8–2.9 V, suggesting good carrier transport capability of these Mn(II) complexes. As shown in Figures 5b and c, the EL spectra of the three Mn(II) complexes exhibit green emission at about 530 nm (CIE = 0.33, 0.57) for DtbuPO-$MnBr_2$, at 525 nm (CIE = 0.32, 0.59) for DcycPO-$MnBr_2$, and yellow-green emission at 540 nm (CIE = 0.36, 0.57) for DPhPO-$MnBr_2$ (Figures 5b-e and S30, Supporting Information). These EL spectra are slightly blue-shifted than the PL spectra in their solid states. The parameters of the devices are summarized in detail in Table S4, Supporting Information. Thus, the optimized device performance with the maximum EQE (EQE_{max}) of 15.7%, power efficiency (PE_{max}) of 53.9 lm W^{-1} and current efficiency (CE_{max}) of 48.1 cd A^{-1} were recorded for DtbuPO-$MnBr_2$, 14.3%, 53.6 lm W^{-1} and 47.8 cd A^{-1} were recorded for DPhPO-$MnBr_2$ and 12.4%, 41.3 lm W^{-1} and 36.8 cd A^{-1} were recorded for DcycPO-$MnBr_2$. To the best of our knowledge, the achieved EQE_{max} value of 15.7% is among the highest values for Mn complex-based OLED so far (Figure 5f and Table S4, Supporting Information).

3. Conclusion

In summary, we have successfully designed an efficient approach to tune the emission color of neutral tetrahedral Mn(II) complexes. Experimental results and theoretical calculations have confirmed that steric hindrance driven bond angle distortion strategy can effectively tune the emission colors of tetrahedral neutral Mn(II) complexes from blue-green to yellow-green. In addition, significant CPL signals can be observed in the single crystals of these achiral Mn(II) complexes. Importantly, we have achieved a high-performance Mn based OLEDs with a record-breaking external quantum efficiency of 15.7% by using three Mn(II) complexes with high PLQYs as dopants. This work provides a design map for constructing multi-color luminescent Mn(II) complexes, shedding lighting on the discovery of relationship between steric hindrance and energy splitting, which facilitates the fast development of multicolor Mn(II) complexes for OLEDs.

[CCDC 2263691, 2263692, 2263693 and 2263694 contain the supplementary crystallographic data for this paper. These data can be obtained free of charge from The Cambridge Crystallographic Data Centre via www.ccdc.cam.ac.uk/data_request/cif.]

Supporting Information

Supporting Information is available from the Wiley Online Library or from the author.

Declaration of Competing Interest

The authors declare no competing financial interests or personal relationships that could have appeared to influence the work reported in this paper.

Acknowledgements

This work was supported by the National Key Technologies R&D Program of China (2022YFE0104100), National Natural Science Foundation of China (62205277, 52222308 and 22135004), ITC Guangdong-Hong Kong Technology Cooperation Funding Scheme (TCFS) (GHP/038/19GD), CAS-Croucher Funding Scheme for Joint Laboratories (ZH4A), the Open Research Fund of State Key Laboratory of Polymer Physics and Chemistry, Changchun Institute of Applied Chemistry, Chinese Academy of Sciences, the Hong Kong Research Grants Council (PolyU 15305320), the Hong Kong Polytechnic University (YXBR), Miss Clarea Au for the Endowed Professorship in Energy (847S), and Research Institute for Smart Energy (CDAQ).

Received: ((will be filled in by the editorial staff))

Revised: ((will be filled in by the editorial staff))

Published online: ((will be filled in by the editorial staff))

References

[1] A. K.-W. Chan, M. Ng, Y.-C. Wong, M.-Y. Chan, W.-T. Wong, V. W.-W. Yam, *J. Am. Chem. Soc.* **2017**, *139*, 10750.

[2] J H.-H. Kuo, Y.-T. Chen, L. R. Devereux, C.-C. Wu, M. A. Fox, C.-Y. Kuei, Y. Chi, G.-H. Lee, *Adv. Mater.* **2017**, *29*, 1702464.

[3] X. Yang, L. Yue, Y. Yu, B. Liu, J. Dang, Y. Sun, G. Zhou, Z. Wu, W.-Y. Wong, *Adv. Optical Mater.* **2020**, *8*, 2000079.

[4] X. Wang, J. Kuang, P. Wu, Z. Zong, Z. Li, H. Wang, J. Li, P. Dai, K. Y. Zhang, S. Liu, W. Huang, Q. Zhao, *Adv. Mater.* **2022**, *34*, 2107013.

[5] H. Yuan, Z. Han, Y. Chen, F. Qi, H. Fang, Z. Guo, S. Zhang, W. He, *Angew. Chem. Int. Ed.* **2021**, *60*, 8174.

[6] K. Y. Zhang, X. Chen, G. Sun, T. Zhang, S. Liu, Q. Zhao, W. Huang, *Adv. Mater.* **2016**, *28*, 7137.

[7] L.-L. Yan, L.-Y. Yao, M. Ng, W. K. Tang, M.-Y. Leung, V. W.-W. Yam, *J. Am. Chem. Soc.* **2022**, *144*, 19748.

[8] J. Li, K. Chen, J. Wei, Y. Ma, R. Zhou, S. Liu, Q. Zhao, W.-Y. Wong, *J. Am. Chem. Soc*. **2021**, *143*, 18317.

[9] X. Feng, J.-G. Yang, J. Miao, C. Zhong, X. Yin, N. Li, C. Wu, Q. Zhang, Y. Chen, K. Li, C. Yang, *Angew. Chem. Int. Ed.* **2022**, *61*, e202209451.

[10] S.-F. Wang, B.-K. Su, X.-Q. Wang, Y.-C. Wei, K.-H. Kuo, C.-H. Wang, S.-H. Liu, L.-S. Liao, W.-Y. Hung, L.-W. Fu, W.-T. Chuang, M. Qin, X. Lu, C. You, Y. Chi, P.-T. Chou, *Nat. Photonics* **2022**, *16*, 843.

[11] L.-J. Xu, C.-Z. Sun, H. Xiao, Y. Wu, Z.-N. Chen, *Adv. Mater.* **2017**, *29*, 1605739.

[12] Y. Qin, P. Tao, L. Gao, P. She, S. Liu, X. Li, F. Li, H. Wang, Q. Zhao, Y. Miao, W. Huang, *Adv. Optical Mater.* **2019**, *7*, 1801160.

[13] S. Yan, W. Tian, H. Chen, K. Tang, T. Lin, G. Zhong, L. Qiu, X. Pan, W. Wang, *Adv. Funct. Mater.* **2021**, *31*, 2100855.

[14] G.-H. Tan, Y.-N. Chen, Y.-T. Chuang, H.-C. Lin, C.-A. Hsieh, Y.-S. Chen, T.-Y. Lee, W.-C. Miao, H.-C. Kuo, L.-Y. Chen, K.-T. Wong, H.-W. Lin, *Small* **2023**, *19*, 2205981.

[15] P. She, Y. Ma, Y. Qin, M. Xie, F. Li, S. Liu, W. Huang, Q. Zhao, *Matter* **2019**, *1*, 1644.

[16] X. Huang, Y. Qin, P. She, H. Meng, S. Liu, Q. Zhao, *Dalton Trans.* **2021**, *50*, 8831.

[17] C. Sun, H. Lu, C.-Y. Yue, H. Fei, S. Wu, S. Wang, X.-W. Lei, *ACS Appl. Mater. Interfaces* **2022**, *14*, 56176.

[18] H. Meng, W. Zhu, F. Li, X. Huang, Y. Qin, S. Liu, Y. Yang, W. Huang, Q. Zhao, *Laser Photonics Rev.* **2021**, *15*, 2100309.

[19] L.-J. Xu, X. Lin, Q. He, M. Worku, B. Ma, *Nat. Commun.* **2020**, *11*, 4329

[20] J.-B. Luo, J.-H. Wei, Z.-Z. Zhang, Z.-L. He, D.-B. Kuang, *Angew. Chem. Int. Ed.* **2023**, *62*, e202216504.

[21] M. P. Davydova, L. Meng, M. I. Rakhmanova, Z. Jia, A. S. Berezin, I. Y. Bagryanskaya, Q. Lin, H. Meng, A. V. Artem'ev, *Adv. Mater.*, https://doi.org/10.1002/adma.202303611.

[22] Y. Xu, Z. Li, G. Peng, F. Qiu, Z. Li, Y. Lei, Y. Deng, H. Wang, Z. Liu, Z. Jin, *Adv. Optical Mater.***2023**, *11*, 2300216.

[23] Q. Guo, W.-Y. Zhang, C. Chen, Q. Ye, D.-W. Fu, *J. Mater. Chem. C* **2017**, *5*, 5458

[24] Y. Qin, P. She, X. Huang, W. Huang, Q. Zhao, *Coord. Chem. Rev.* **2020**, *416*, 213331.

[25] P. Tao, S.-J. Liu, W.-Y. Wong, *Adv. Optical Mater.* **2020**, *8*, 2000985.

[26] Y. Wu, X. Zhang, L.-J. Xu, M. Yang, Z.-N. Chen, *Inorg. Chem.* **2018**, *57*, 9175.

[27] V. Morad, I. Cherniukh, L. Pöttschacher, Y. Shynkarenko, S. Yakunin, M. V. Kovalenko, *Chem. Mater.* **2019**, *31*, 10161.

[28] J. Chen, S. Zhang, X. Pan, R. Li, S. Ye, A. K. Cheetham, L. Mao, *Angew. Chem. Int. Ed.* **2022**, *61*, e202205906.

[29] X. Zhao, M. Wu, H. Liu, Y. Wang, K. Wang, X. Yang, B. Zou, *Adv. Funct. Mater.* **2022**, *32*, 2109277.

[30] Q. Ren, J. Zhang, Y. Mao, M. S. Molokeev, G. Zhou, X.-M. Zhang, *Nanomaterials* **2022**, *12*, 3142.

[31] S. Zhang, Y. Zhao, Y. Zhou, M. Li, W. Wang, H. Ming, X. Jing, S. Ye, *J. Phys. Chem. Lett.* **2021**, *12*, 8692.

[32] M. P. Davydova, L. Meng, M. I. Rakhmanova, I. Y. Bagryanskaya, V. S. Sulyaeva, H. Meng, A. V. Artem'ev, *Adv. Optical Mater.* **2023**, *11*, 2202811.

[33] G. E. Hardy, J. I. Zink, *Inorg. Chem.* **1976**, *15*, 3061.

[34] A. V. Artem'ev, M. P. Davydova, A. S. Berezin, D. G. Samsonenko, I. Y. Bagryanskaya, V. K. Brel, X. Hei, K. A. Brylev, O. I. Artyushin, L. E. Zelenkov, I. I. Shishkin, J. Li, *ACS Appl. Mater. Interfaces* **2022**, *14*, 31000.

[35] A. V. Artem'ev, M. P. Davydova, M. I. Rakhmanova, I. Y. Bagryanskaya, D. P. Pishchur, *Inorg. Chem. Front.* **2021**, *8*, 3767.

[36] D. L. Dexter, *J. Chem. Phys.* **1953**, *21*, 836.

[37] Z. Dou, J. Yu, Y. Cui, Y. Yang, Z. Wang, D. Yang, G. Qian, *J. Am. Chem. Soc.* **2014**, *136*, 5527.

[38] T. Lu, Q. Chen, *Journal of Computational Chemistry* **2022**, *43*, 539.

[39] M. Liu, L. Zhang, T. Wang, *Chem. Rev.* **2015**, *115*, 7304.

[40] L.-L. Xu, H.-F. Zhang, M. Li, S. W. Ng, J.-H. Feng, J.-G. Mao, D. Li, *J. Am. Chem. Soc.* **2018**, *140*, 11569.

[41] J. Zhao, T. Zhang, X.-Y. Dong, M.-E. Sun, C. Zhang, X. Li, Y. S. Zhao, S.-Q. Zang, *J. Am. Chem. Soc.* **2019**, *141*, 15755.

[42] K. S. Yook, J. Y. Lee, *Adv. Mater.* **2014**, *26*, 4218.